# EVALUATION OF THE CAMS GRIDDED SOLAR RADIATION MODEL IN BRAZIL

**João Marcos Oliveira de Senna Caaetê Chacon[1], Olga de Castro Vilela[1], Diego Rodrigues de Miranda[2], Faiza Azam[2]**

[1] Universidade Federal de Pernambuco (UFPE), Center of Renewable Energies, Recife (Brazil)

[2] German Aerospace Center (DLR), Institute of Networked Energy Systems, Oldenburg (Germany)

**Abstract**

This study provides an evaluation of the Copernicus Atmosphere Monitoring Service (CAMS) Radiation Service (CRS) gridded solar radiation model for the Brazilian territory, focusing on its application for detailed spatiotemporal analyses. The research validates an extensive 19-year dataset of CAMS solar radiation estimations (2005-2023) by performing a rigorous comparison against high-quality ground-based measurements from 11 stations geographically dispersed throughout the country. Beyond simple pointwise comparisons, this work critically explores the model's capability to represent complex geographical and climatic patterns through the generation of monthly solar radiation anomaly and long-term trend maps. The methodology employed a multi-step process including bilinear interpolation to align the gridded satellite data with precise station coordinates, the calculation of statistical metrics (nMBE, nRMSE) across multiple time scales, and a comprehensive seasonal analysis. The resulting maps successfully revealed significant spatial variations in solar radiation directly linked to large-scale climatic phenomena, as the El Niño-Southern Oscillation (ENSO), underscoring the utility of CAMS data for regional-scale climate studies. The conclusion emphasizes the potential of CAMS as a promising and valuable tool for solar radiation mapping, while also acknowledging the inherent challenges in fully representing highly localized atmospheric conditions. The approach demonstrates how gridded models can effectively complement and extend in-situ measurements, particularly in vast regions with limited ground data availability.

*Keywords: Solar radiation, CAMS, gridded maps, validation, Brazil, spatiotemporal analysis, solar energy.*

## 1. Introduction

Solar radiation stands as one of the most abundant and widely distributed energy sources on the planet, and consequently, the deployment of solar energy systems is experiencing exponential growth worldwide. This global expansion is primarily fuelled by two synergistic factors: a heightened awareness of environmental sustainability and unprecedented reductions in the costs of solar photovoltaic systems. According to the International Renewable Energy Agency (IRENA, 2024), as seen in Figure 1, the average price of solar modules has plummeted by over 87% since 2010, rendering solar energy not only more accessible but also highly competitive against traditional energy sources. This transformative shift plays a crucial role in the ongoing global energy transition, offering solar energy as a clean, scalable, and sustainable alternative.


10.18086/swc.2025.04.22 Available at http://proceedings.ises.org

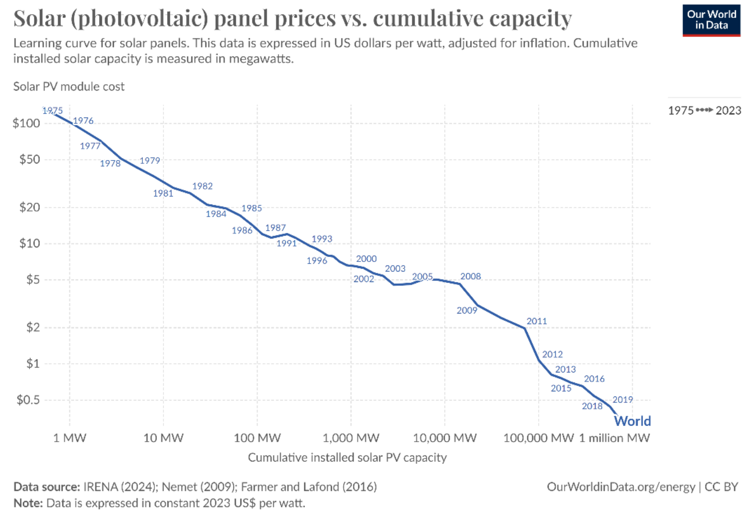


**Figure 1: PV Panel x Global Solar Capacity. Source: IRENA (2024); Nemet (2009); Farmer and Lafond (2016) by Our World in Data.**

Despite these advancements, the inherent variability and intermittency of the solar resource present significant challenges for energy systems, particularly concerning grid stability and reliability. Fluctuations in solar radiation are attributed to a complex interplay of meteorological factors, including cloud cover, atmospheric aerosols, and water vapor content. Therefore, a detailed and accurate characterization of the solar resource is essential for assessing the solar potential of different regions, optimizing the design of solar power plants, and forecasting energy production.

In this context, satellite-derived solar radiation databases have become indispensable tools in solar irradiation study (Huang et al., 2019). This work focuses on the comprehensive evaluation of an extensive solar irradiance dataset provided by the Copernicus Atmosphere Monitoring Service (CAMS), a component of Europe's Earth observation program, through its Radiation Service (CRS). The CRS contains a continuous 19-year record of data, offering invaluable insights into the spatial distribution and temporal variability of solar radiation. For simplicity the CAMS Radiation Service will be referred in this work as CAMS.

The primary objective of this study is to validate the quality and reliability of the CAMS gridded solar radiation data for the Brazilian territory. This is achieved by systematically comparing the satellite-derived estimations with high-quality ground measurements from 11 stations strategically located across Brazil's diverse climates. Beyond a simple statistical validation, this paper aims to analyse the long-term progression of radiation levels, focusing on percentage variations and their geographic distribution. By investigating this historical dataset, we aim to identify regions that have experienced significant changes in radiation levels over time, effectively creating a dynamic analysis of trends and patterns that can complement static resources like a solar atlas.

## 2. CAMS Gridded Solar Radiation Dataset

Copernicus Atmosphere Monitoring Service (CAMS) is part of the Europea's Earth observation services and provides consistent, quality-controlled information related to air pollution and health, solar energy, greenhouse gases and climate behaviour (CAMS, 2025). CAMS offers CRS as a supplementary service with solar radiation time series as its primary product which is widely used for energy systems analysis. In addition, it provides gridded data for energy system analysis on a spatial scale.

Time series in 1 min, 15 min, hourly and daily temporal resolution are calculated 'on-the-fly' on user request at the desired location using the information on clouds from geostationary satellites as Meteosat Second Generation (MSG) and Himawari. MSG primarily covers Europe and Africa, extending into adjacent regions such as parts of South America and the Middle East, while Himawari provides coverage over East and Southeast Asia, Oceania, and the western Pacific region. Together, these satellites ensure continuous monitoring of cloud properties over large portions of the Eastern Hemisphere, enabling robust solar radiation estimations.

Furthermore, to the standard access as single time series at the user's individual target location, a gridded dataset for land surfaces of Europe and Africa and parts of Asia for the MSG field of view (FOV) and for the Asia_Oceanica region in the Himawari FOV is available. This is based on a retrieved collection of many time series in a 0.1° spatial grid and in a 15 min temporal resolution which are restructured to a gridded monthly data file as illustrated in Figure

2, in netCDF format.

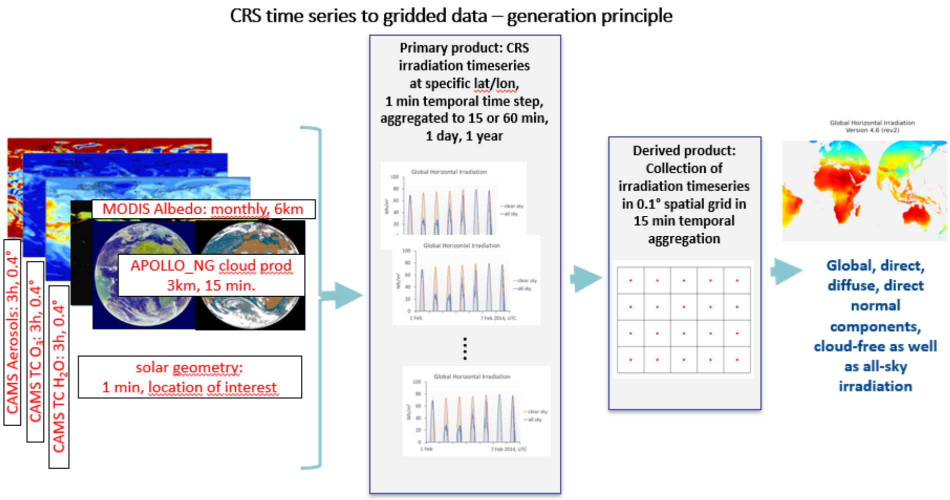


**Figure 2: The general principle of CRS gridded data. Source: F. Azam, Personal Communication, 31.03.2025.**

The dataset of our interest is for the MSG FOV, which spans from January 2005 to December 2023 and provides key irradiance components essential for solar energy analysis. These include Global Horizontal Irradiation (GHI), the global radiation on a horizontal surface; Beam Normal Irradiation (BNI), representing direct radiation perpendicular to the sun's rays; Beam Horizontal Irradiation (BHI), the direct component on a horizontal plane; and Diffuse Horizontal Irradiation (DHI), the scattered component of radiation. Data is available for both modelled clear-sky conditions, which are calculated based on atmospheric components like aerosols, ozone, and water vapor, and all-sky conditions, which account for the presence of clouds.

The CAMS Gridded Solar Radiation product offers several advantages over the CAMS Time Series product, providing greater flexibility for a wide range of applications. The CAMS Time Series product delivers more detailed information at a single point and at a higher temporal resolution than 15 min. It's important to note that all the detailed information provided by the CAMS Time Series product is derived from temporal and spatial interpolation on the points between the satellite measurements temporal resolution and modelled atmospheric parameters (Schroedter-Homscheidt et al., 2021).

The gridded format product offers data points across a continuous spatial grid and enables users to apply their own interpolation models to fill in gaps or enhance the resolution of the data, even allowing the use of multi-source data for the modelling (Şen and Şahİn, 2001). Moreover, customized modelling, such as the use of advanced machine learning or physics-based models, can be applied to better understand the spatial relation of solar radiation in a certain area, increasing the accuracy of forecast models in the region, and even supporting more informed decisions in other sectors such as agriculture and environmental management (Vestnik, 2013).

## 3. Methodology

After downloading the CAMS data from CAMS atmospheric data store (ADS), an initial pre-processing stage was conducted to harmonize the dataset for analysis. First, to reduce the computational burden, the data was spatially subset from its original global grid to a rectangular area encompassing Brazil, defined by the coordinates -36º to 10º latitude and -61º to -32º longitude. Subsequently, a temporal adjustment was necessary to align the different time resolutions of the data sources. While the ground-based observational data was available at a one-minute interval, the CAMS gridded dataset provided values every 15 minutes. To ensure consistency, the ground-based time series was resampled to match the timestamps of the gridded data by computing the mean for each corresponding time step. The end of the interval was considered in the timestamp labelling.

To enable a direct comparison with ground-based station data, first a bilinear interpolation was performed on the CAMS gridded product. This spatial interpolation used the four surrounding grid points to generate a satellite-derived time series that precisely matches the latitude and longitude of each measurement station. With the data spatially aligned, a statistical analysis was conducted using the Mean Bias Error (MBE) (Equation 1), the Root Mean Square Error (RMSE) (Equation 2), and the Pearson Correlation Coefficient (Equation 3). To facilitate a more robust comparison across different conditions, normalised mean bias error (nMBE – Equation 4) and normalised root mean square error (nRMSE – Equation 5) were also calculated based on the average of the measured data.

$$MBE = \overline{X} - \overline{Y} \quad \text{(eq. 1)}$$

$$RMSE = \sqrt{\frac{1}{n}\sum_{i=1}^{n}(X - Y)^2} \quad \text{(eq. 2)}$$

$$\rho = \sqrt{\frac{cov(X,Y)}{cov(X,X) \cdot cov(Y,Y)}} \quad \text{(eq. 3)}$$

$$\text{n}MBE = \frac{MBE}{\overline{X}} \quad \text{(eq. 4)}$$

$$nRMSE = \frac{RMSE}{\overline{X}} \quad \text{(eq. 5)}$$

Where X stands for the ground observations and $\overline{X}$ its average, while Y stands for the CAMS model time-series and $\overline{Y}$ its average. For a comprehensive evaluation, the data comparison was performed across multiple temporal aggregations: 15-minute, daily, and monthly time steps. Statistics were gathered for each year to determine if the quality of the CAMS data shows any tendency to improve over the long term. Furthermore, the analysis was segmented by season to assess the influence of different climatic conditions on the product's accuracy. In parallel, the CAMS time-series product was also evaluated against the same ground data to highlight the differences in performance between the directly interpolated gridded data and the on-demand time-series product processed by CAMS.

A multitude of sources were used in the collection of ground data, including the Sistema de Organização Nacional de Dados Ambientais (SONDA) from the Instituto Nacional de Pesquisas Espaciais (INPE), the Baseline Surface Radiation Network (BSRN, Driemel et al., 2018), and the data collection carried by experts of IEA PVPS Task 16 (Forstinger et al., 2023). In total, eleven stations were used, which are listed below in Table 1. The table also provides latitude, longitude, altitude, the period of the measured data and the average daily radiation of the measured series. The climates of each location in Köppen-Geiger classification are also provided. The spatial distribution of the stations can be observed in Figure 3, where they are indicated on the map.

**Table 1: List of Ground Measurement Stations Used for Validation**

| Station | Latitude | Longitude | Altitude (m) | Daily Means (kWh/m²) | Period | Climate |
|---|---|---|---|---|---|---|
| Petrolina | -9.07 | -40.32 | 387 | 5.51 | Mar2008 to Dec2020 | Hot Semi-Arid |
| São Luiz | -2.59 | -44.21 | 40 | 4.84 | Jan2007 to Apr2019 | Tropical Savanna |
| São Martinho da Serra | -29.44 | -53.82 | 489 | 4.79 | Apr2006 to Jun2017 | Humid Subtropical |
| Ourinhos | -22.95 | -49.89 | 446 | 4.80 | Feb2006 to Apr2019 | Humid Subtropical |
| Brasília | -15.60 | -47.71 | 1023 | 5.40 | Feb2006 to Apr2019 | Tropical Savanna |
| Natal | -5.84 | -35.21 | 58 | 5.80 | Jan2015 to Dec2019 | Tropical Savanna |
| Cachoeira Paulista | -22.69 | -45.01 | 574 | 4.93 | Jan2015 to Dec2019 | Humid Subtropical |
| Florianópolis | -27.60 | -48.52 | 31 | 4.27 | Sep2013 to Dec2022 | Humid Subtropical |
| Patos | -7.01 | -37.30 | 267 | 6.23 | Apr2012 to Dec2018 | Hot Semi-Arid |
| Coremas | -7.02 | -37.94 | 239 | 6,15 | Sep2012 to Aug2019 | Tropical Savanna |
| São João do Rio do Peixe | -6.73 | -38.45 | 251 | 6,28 | Sep2012 to Jan2019 | Tropical Savanna |


**Figure 3: Stations in Map. Source: Google My Maps, 2025.**

Following the collection of the measured data, a quality control (QC) process to ensure the exclusion of erroneous data from the evaluation was conducted as described in Miranda et al. (2022). The tests were conducted in accordance with the recommendations of the Baseline Surface Radiation Network (BSRN), ensuring the data met established physical and statistical limits. This multi-step procedure included physically feasible and extremely rare limit tests to check if values were within expected ranges, consistency checks between different radiation components (such as the ratio between global radiation and the sum of direct and diffuse components), and further tests to identify tracker malfunctions and data instability. These checks allowed for a progressive detection of errors and minimizing the impact of missing or invalid values on subsequent analyses. In Figure 4 the percentage of anomalous values for each station in the GHI, DNI and DHI are shown.

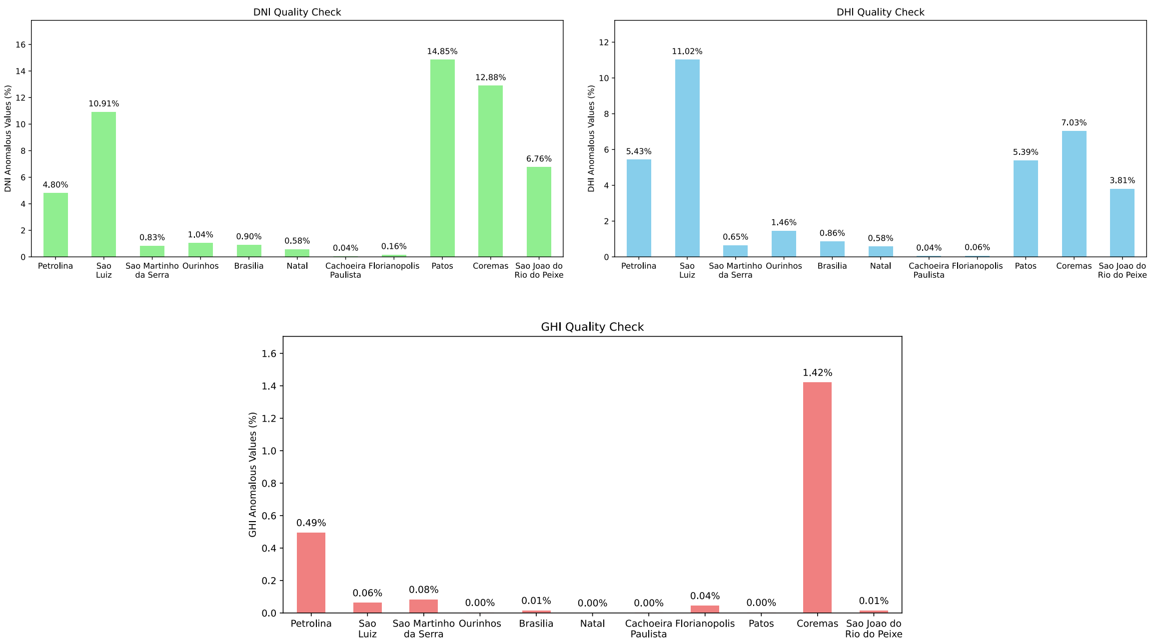


**Figure 4: DNI, DHI and GHI Quality Check. Source: Own Authorship, 2025.**

All the methodology described above, together with the anomaly map generation processes described below are illustrated in, the flowchart shown in Figure 5, presenting the full procedure followed for the analysis.

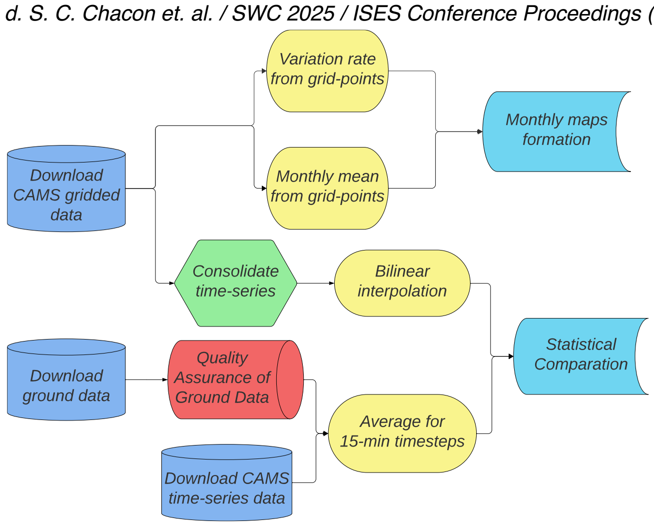


**Figure 5: Methodology Flowchart. Source: Own Authorship, 2025.**

## 3.1. Maps Formation

The validation of CAMS Gridded Radiation data facilitates the analysis of long-term variations in solar radiation across Brazil (INPE, 2017). The validated CAMS gridded data was used to identify spatial and temporal patterns in radiation anomalies. The data used for the map is the Global Horizontal Irradiance (GHI) structured on a geographical grid covering Brazil. The initial step entailed the computation of the historical monthly mean for each grid point. This was achieved by selecting all radiation values corresponding to a specific month across the 19-year period followed by calculating the average daily radiation for that month. This resulted in 12 reference datasets, one for each calendar month. The purpose of this approach was to create a baseline that accounts for seasonal variations, allowing for a more accurate assessment of deviations from expected radiation levels. This resulted in twelve reference datasets that account for seasonal variations. Subsequently, these historical means were used to calculate the percentage anomaly for each month by comparing the observed radiation values with the corresponding historical mean, as detailed in Equation 6 (Costa et al., 2018):

$$\text{Anomaly (\%)} = 100 \times \frac{\text{Observed Radiation} - \text{Historical Mean}}{\text{Historical Mean}} \qquad \text{(eq. 6)}$$

This anomaly calculation was applied to every grid point, generating spatial matrices of percentage variation that were then visualized as anomaly maps, as shown in the example for January 2005 (Figure 6) and the monthly climatology for the same month (Figure 7). These maps facilitate an in-depth evaluation of solar radiation variability, allowing for the identification of seasonal patterns, extreme variations, and potential long-term trends. To further observe the progression of solar radiation over the years, a more precise trend analysis was conducted by calculating the trend line for each grid point separately for each month. By determining the rate of change in Wh/year, this approach provides detailed insights into seasonal and long-term trends, allowing for the generation of maps that visually represent the spatial and temporal distribution of these changes.

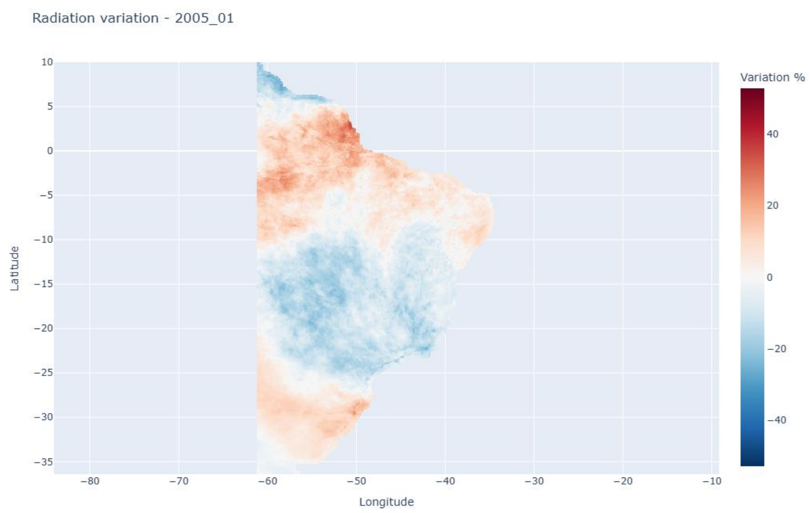

**Figure 6: Anomaly Map in January 2005. Source: Own Authorship, 2025.**

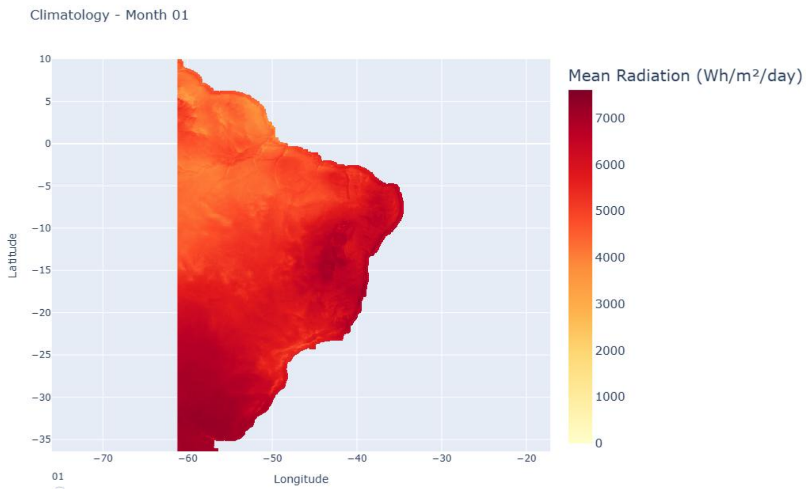


**Figure 7: Climatology Maps. Source: Own Authorship, 2025.**

In addition, to observe more precisely the progression of solar radiation over the years for each region, the trend lines of each point were analysed separately for each month of the year, observing the variation rate of these lines. This approach allows for a detailed analysis of how solar radiation changes every month, providing insights into seasonal variations and long-term trends (Pons and Ninyerola, 2008; Wilcox and Gueymard, 2010; Qi et al., 2024; Correa et al., 2024). By calculating the rate of change in Wh/year for each point, we can generate maps that visually represent the spatial and temporal distribution of these changes. The trend line for each point, derived from the monthly data, serves as a critical tool for understanding the dynamics of solar radiation over time. The generation of these maps, which incorporate the rate of change in Wh/year, provides a powerful visual representation of the data for specific months, allowing for a detailed examination of how these trends vary across different regions. A positive trend indicates that the solar radiation during that month has historically increased over the years (2005-2023), while a negative trend indicates a decrease in radiation values over time. By separating the data by month, we can better understand the seasonal influences on solar radiation and how these influences may be changing over time.

## 4. Results and conclusions

The statistical results generally indicate that the CAMS model tends to overestimate solar radiation compared to ground-based measurements for monthly statistics, as shown by the negative nMBE values in Figure 8. However, an exception is noted at the São Martinho da Serra station, where a more balanced agreement between the model and measured data is observed. The deviations shown by the nRMSE values (Figure 9) may be attributed to local atmospheric conditions, surface features, or specific characteristics of the station's measurement setup. To better ascertain how local climate affects model performance, the stations in the figures are intentionally sorted by their average annual daily GHI radiation (from lowest to highest, as detailed in Table 1).

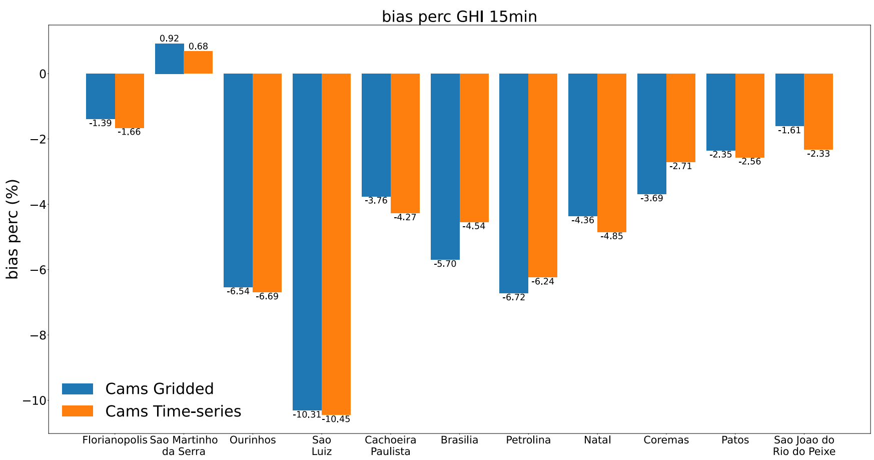


**Figure 8: GHI nMBE (%) for 15-min time resolution. Source: Own Authorship, 2025**

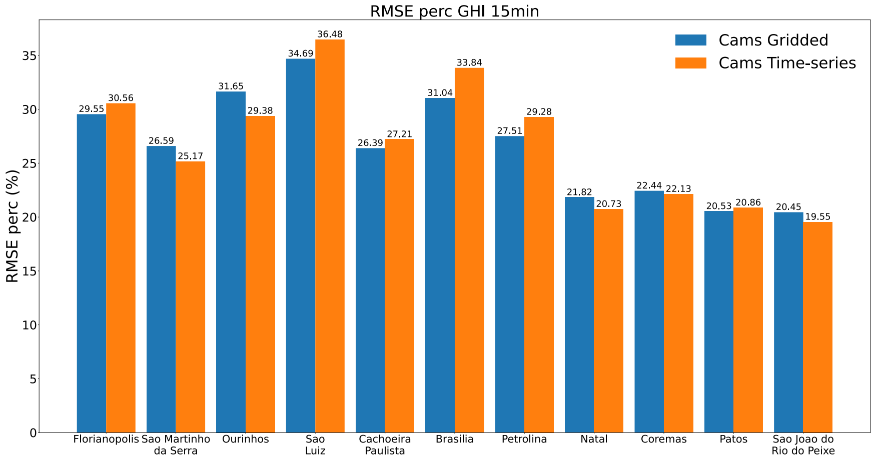


**Figure 9: GHI nRMSE (%) for 15-min time resolution. Source: Own Authorship, 2025**

A comparative analysis of the radiation components reveals that the GHI from CAMS is considerably more accurate, with a nRMSE of approximately 30%. In contrast, the DHI and DNI from CAMS show larger deviations, with errors around 50%, as seen in Figures 10 and 11, respectively. This highlights the challenges in modeling these more sensitive components of solar radiation. A key aspect of this study was the comparison between the CAMS Gridded data, processed with bilinear interpolation, and the point-specific CAMS Time Series. Although bilinear interpolation is a relatively simple method, the overall nRMSE results for both products were generally similar. However, the relative performance varied by location, underscoring the necessity of carefully selecting data sources and interpolation methodologies based on the specific application and regional characteristics.

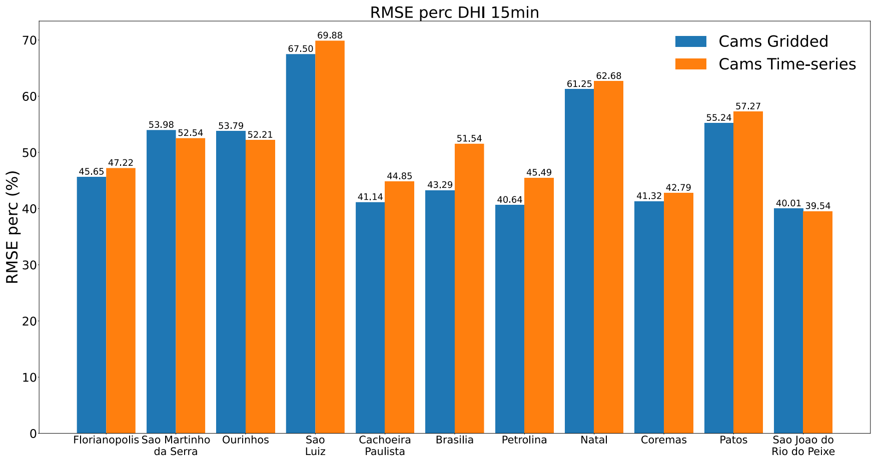


**Figure 10: DHI nRMSE (%) for 15-min time resolution. Source: Own Authorship, 2025.**

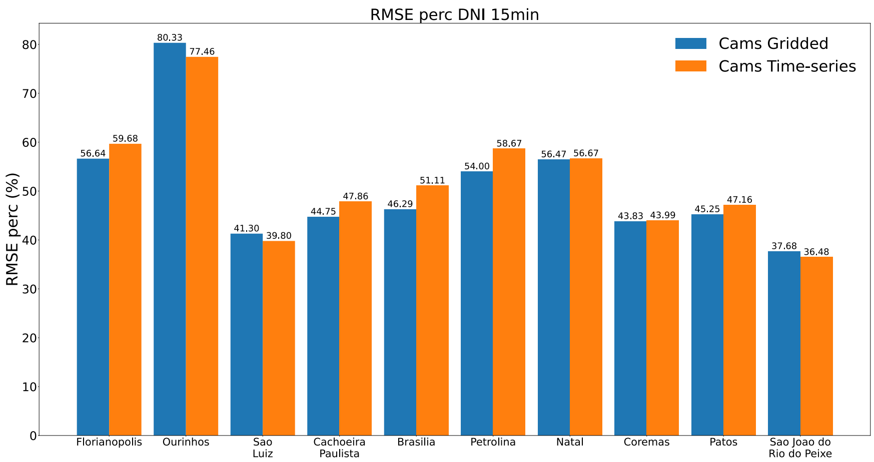


**Figure 11: DNI nRMSE (%) for 15-min time resolution. Source: Own Authorship, 2025.**

The analysis also identified a strong influence of temporal resolution and seasonal patterns on model accuracy. A clear seasonal variation in error was observed, with higher discrepancies during the summer and early autumn. This period is characterized by increased cloud cover across much of Brazil, which directly impacts solar radiation levels, a trend that is illustrated in Figure 12, which the percentage of time the sky is clear, mostly clear, or partly cloudy (i.e., less than 60% of the sky is covered by clouds) according to the Weather Spark database. Then, lower percentages indicate higher cloud cover which is likely higher in the period from November until beginning of March.

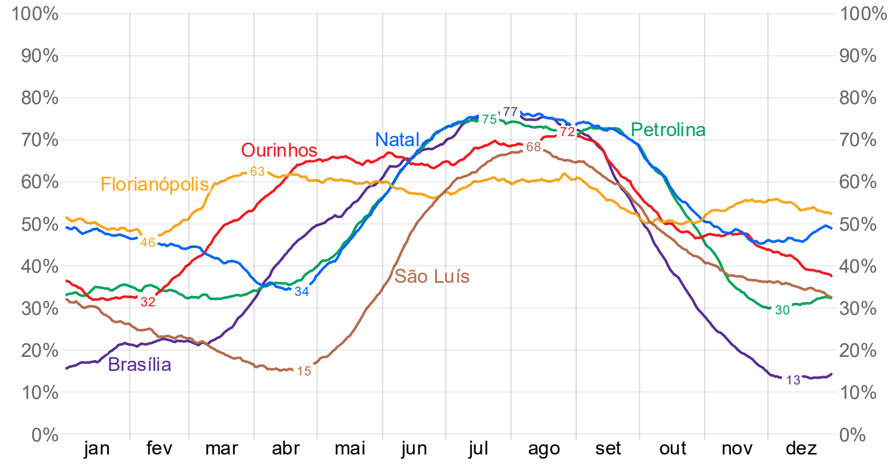


**Figure 12: Chances of Clearer Sky. Source: Adapted from Weather Spark database, 2025.**

The case study of the Petrolina station in Figure 13, where the yellow bars represent summer and the blue bars represent winter, illustrates this seasonal pattern, which is further reinforced by the aggregated seasonal data for all stations, presented in Figures 14 and 15. Furthermore, model errors were significantly smaller when data was aggregated from a 15-minute resolution to daily or monthly scales. This is an expected outcome, as short-term fluctuations caused by transient weather events tend to cancel out over longer time intervals, resulting in a more stable representation of radiation levels.

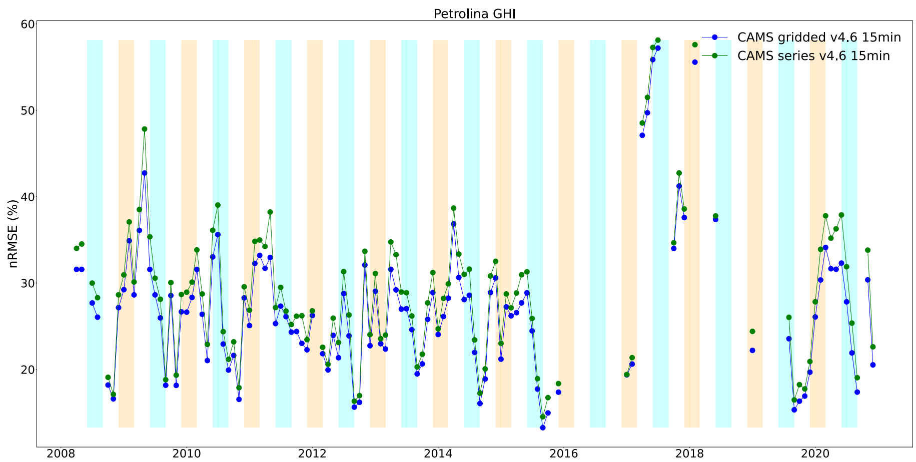


**Figure 13: Monthly GHI nRMSE (%) for Petrolina. Source: Own Authorship, 2025.**

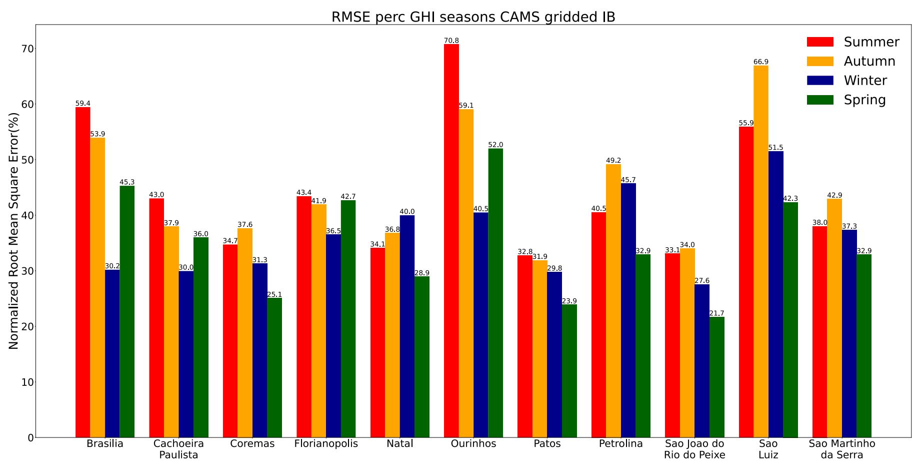


**Figure 14: Seasons nRMSE GHI CAMS gridded. Source: Own Authorship, 2025.**

### 4.1. Radiation Maps

The CAMS gridded dataset enables the creation of anomaly and trend maps, providing a visual analysis of spatiotemporal solar radiation variations across Brazil. The analysis of the anomaly maps revealed a distinct pattern associated with the El Niño-Southern Oscillation (ENSO) phases, whose recent cycles are depicted in the Oceanic Niño Index (ONI) shown in Figure 15. During moderate to strong El Niño events, such as those in late 2015 and 2023 shown in Figure 16, a clear discrepancy was observed: the central and northeastern regions exhibited positive anomalies (increased radiation), while the southern region displayed negative anomalies (reduced radiation). This pattern is consistent with the known effects of El Niño, which tends to cause drought conditions and clearer skies in the northeast while bringing more intense rainfall and cloud cover to the south. In contrast, during strong to moderate La Niña phases, such as in late 2010 and 2020 shown in Figure 17, the variation in radiation tends to be more homogenous throughout the country, balancing out the typical differences between the north and south of Brazil. These observations highlight the importance of considering ENSO phases when analysing long-term variations in solar radiation, as the differences between El Niño and La Niña periods underscore the role of large-scale climatic phenomena in modulating solar energy variability.

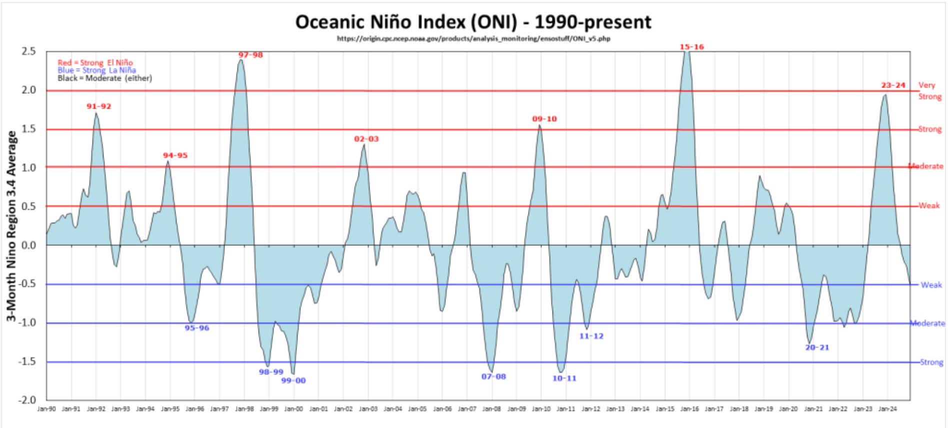


**Figure 15: Oceanic Niño Index (ONI). Source: GG Weather, accessed on 28 Mar 2025.**

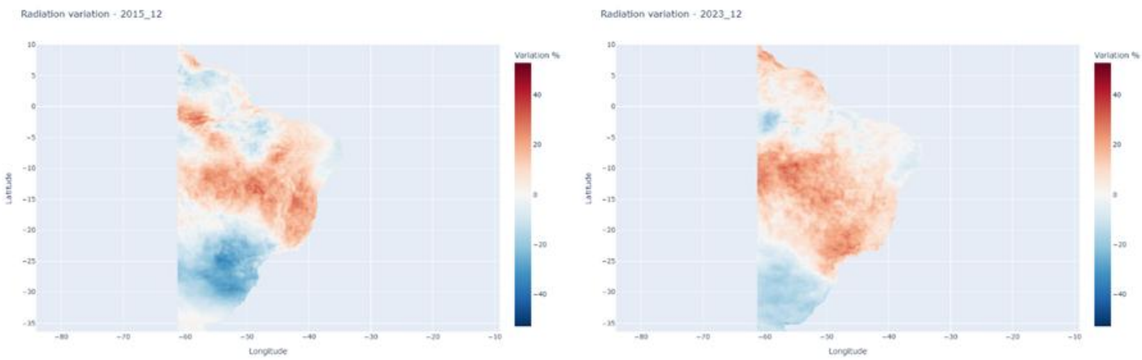


**Figure 16: Anomaly Maps for December 2015 and 2023. Source: Own Authorship, 2025.**

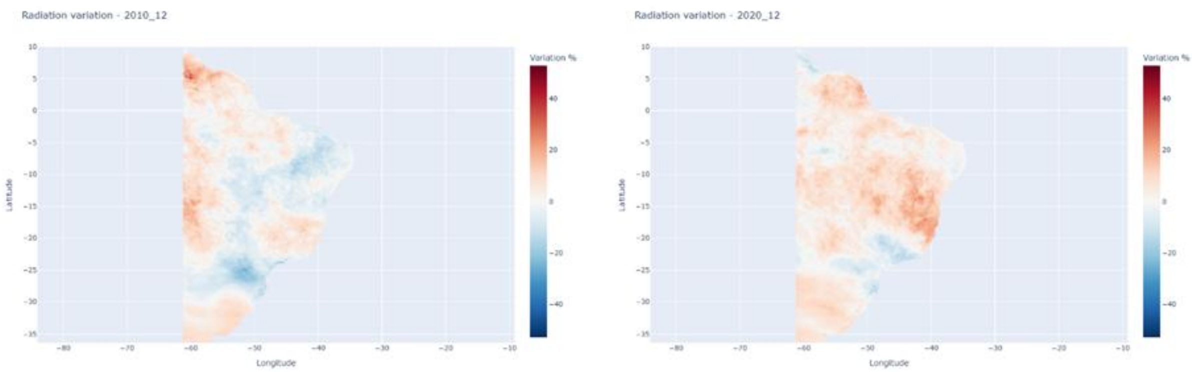


**Figure 17: Anomaly Maps for December 2010 and 2020. Source: Own Authorship, 2025.**

In addition to anomalies, trend maps were generated to analyse the rate of change in solar radiation over the 19-year study period. A distinct spatial pattern emerged, showing a region of predominantly positive variation—indicating a systematic increase in solar radiation—extending from the Southeast towards the Central and Northern areas of Brazil, as exemplified by the trend map for January in Figure 18. This long-term trend may be influenced by large-scale meteorological systems such as the South Atlantic Convergence Zone (SACZ). Understanding these historical trends and anomalies is essential for both energy planning and climate studies, as it provides critical information on the spatial and temporal distribution of solar resources.

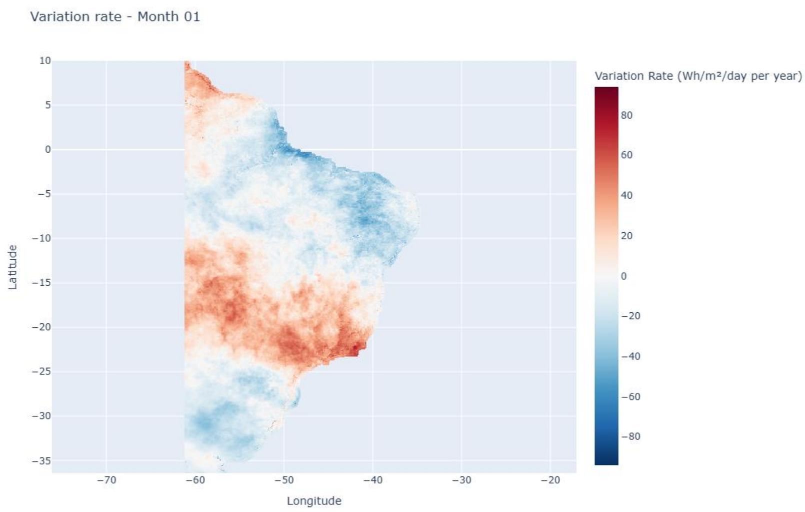


**Figure 18: Trend Map for January. Source: Own Authorship, 2025.**

To enhance the accuracy and reliability of the CAMS Radiation Service, future investigations should focus on critical methodological improvements. A key area of focus is the integration of hybrid models that combine satellite data with real-time ground measurements. Furthermore, it is essential to incorporate dynamic correction factors for cloud cover and atmospheric scattering. The implementation of these enhancements is expected to further increase the capacity of the CAMS gridded radiation database to account for local variations, which is particularly important in regions characterized by significant weather variability. The continued effectiveness of the database in supporting the planning and development of solar energy projects in Brazil and beyond relies on the incorporation of these additional data sources or correction methods.

## 5. Acknowledgments

The authors gratefully acknowledge the CAMS Radiation Service for providing the solar radiation modeled time-series and gridded dataset within the Copernicus Atmosphere Monitoring Service (CAMS) Atmosphere Data Store (ADS), available in https://ads.atmosphere.copernicus.eu/cdsapp#!/dataset/cams-solar-radiation-timeseries?tab=overview. The authors also thank all operators of the ground stations of the BSRN and SONDA networks for their valuable measurements, and also the efforts of the IEA PVPS Task 16 researchers in building the data collection from different radiation networks. We extend our sincere gratitude to São Francisco Hydroelectric Company (CHESF-ELETROBRAS) for their support through the CHESF-CASANOVA project, ANEEL CODE: PD-00048-0217.

## 6. References

COPERNICUS ATMOSPHERE MONITORING SERVICE (CAMS), 2025a. CAMS gridded solar radiation. Atmosphere Data Store (ADS). https://ads.atmosphere.copernicus.eu/datasets/cams-gridded-solar-radiation?tab=overview (accessed 15 January 2025).

COPERNICUS ATMOSPHERE MONITORING SERVICE (CAMS), 2025b. CAMS solar radiation time-series. Atmosphere Data Store (ADS). https://ads.atmosphere.copernicus.eu/datasets/cams-solar-radiation-timeseries?tab=overview (accessed 15 January 2025).

COPERNICUS ATMOSPHERE MONITORING SERVICE, 2025. Copernicus Atmosphere Monitoring Service. https://atmosphere.copernicus.eu (accessed 15 January 2025).

Costa, R. C., Silva, J. R., & Pereira, L. F. (2018). *Mapping of solar radiation anomalies based on climate change*. *Revista Brasileira de Geografia Física*, 11(5), 1502–1515. Available at: https://scispace.com/pdf/mapping-of-solar-radiation-anomalies-based-on-climate-change-49bl8nvhr1.pdf

Driemel, A.; Augustine, J.; Behrens, K.; Colle, S.; Cox, C.; Cuevas-Agulló, E.; Denn, F.M.; Duprat, T.; Fukuda, M.; Grobe, H.; Haeffelin, M.; Hodges, G.; Hyett, N.; Ijima, O.; Kallis, A.; Knap, W.; Kustov, V.; Long, C.N.; Longenecker, D.; Lupi, A.; Maturilli, M.; Mimouni, M.; Ntsangwane, L.; Ogihara, H.; Olano, X.; Olefs, M.; Omori, M.; Passamani, L.; Pereira, E.B.; Schmithüsen, H.; Schumacher, S.; Sieger, R.; Tamlyn, J.; Yogt, R.; Yuilleumier, L.; Xia, X.; Ohmura, A.; König-Langlo, G. Baseline Surface Radiation Network (BSRN): structure and data description (1992–2017). Earth Syst. Sci. Data 10 (3), 1491–1501, https://doi.org/10.5194/essd-10-1491-2018, 2018.

Farmer, J. D., & Lafond, F. (2016). *How predictable is technological progress? Research Policy*, 45(3), 647–665. https://doi.org/10.1016/j.respol.2015.11.001

Ferreira Correa, L., Folini, D., Chtirkova, B., Wild, M., 2024. Trends in observed surface solar radiation and their causes in Brazil in the first two decades of the 21st century. Atmos. Chem. Phys. 24, 8797-8819. https://doi.org/10.5194/acp-24-8797-2024

Forstinger, A.; Wilbert, S.; Jensen, A.; Kraas, B.; Fernández-peruchena, Carlos M.; Gueymard, C.; Ronzio, D.; Yang, D.; Collino, E.; Polo, J.; Ruiz-Arias, J.; Blanc, P.; Saint-Drenan, Yves-M. Worldwide Benchmark of Modelled Solar Irradiance Data 2023 PVPS Task 16 Solar Resource for High Penetration and Large Scale, Report IEA-PVPS T16-05, ISBN 978-3-907281-44-44, 2023.

GG WEATHER, 2025. Oceanic Niño Index (ONI) ENSO. https://ggweather.com/enso/oni.htm (accessed 28 March 2025).

GOOGLE MAPS, 2025. Custom Map Viewer. https://www.google.com/maps/d (accessed 14 February 2025).

Huang, G.; Li, Z.; Li, X.; Liang, S.; Yang, K.; Wang, D.; Zhang, Y. Estimating Surface Solar Irradiance from Satellites: Past, Present, and Future Perspectives. Remote Sensing of Environment, 233, 111371, 2019.

IRENA (2025). *Renewable Power Generation Costs in 2024*. International Renewable Energy Agency. Available at: https://www.irena.org

Kobler, A., Zupan, S., Kocjan, A., 2013. Comparison of spatial interpolation methods and multi-layer neural networks for different point distributions on a digital elevation model. Geodetski Vestnik 57, 523-543. http://doi.org/10.15292/geodetski-vestnik.2013.03.523-543

Miranda, D. R., Petribú, L.; Galdino, J. J. B.; Furtado, J. V.; Barboza, L., Vilela, O. C.; Costa, A. C: A.; Gomes, E.; Pereira, A.; Jatobá, E.; Neto, A. C.; Filho, J. B. Quality Assurance Procedure for Solar Radiation at Minute Resolution. EuroSun 2022: 14th International Conference on Solar Energy for Buildings and Industry, 25-29 Sep. 2022, Kassel, Germany, doi: 10.18086/eurosun.2022.15.04, 2022.

Nemet, G. F. (2009). *Interim monitoring of cost dynamics for publicly supported energy technologies*. *Energy Policy*, 37(3), 825–835. https://doi.org/10.1016/j.enpol.2008.10.041

Our World In Data, 2024. Solar photovoltaic module price. https://ourworldindata.org/grapher/solar-pv-prices-vs-cumulative-capacity (accessed 18 January 2025).

Pereira, E.B., et al., 2017. Atlas Brasileiro de Energia Solar, second ed. INPE, São José dos Campos. http://doi.org/10.34024/978851700089

Pons, X., Ninyerola, M., 2008. Mapping a topographic global solar radiation model implemented in a GIS and refined with ground data. Int. J. Climatol. 28, 1821-1834. https://doi.org/10.1002/joc.1676

Qi, Q., et al., 2024. Mapping of 10-km daily diffuse solar radiation across China from reanalysis data and a Machine-Learning method. Sci. Data 11, 756. https://doi.org/10.1038/s41597-024-03609-1

Schroedter-Homscheidt, M., et al., 2021. User's Guide to the CAMS Radiation Service (CRS) Status December 2021. https://atmosphere.copernicus.eu/sites/default/files/2022-01/CAMS2 73 2021SC1 D3.2.1 2021 UserGuide v1.pdf (accessed 31 March 2025).

Şen, Z., Şahin, A.D., 2001. Spatial interpolation and estimation of solar irradiation by cumulative semivariograms. Sol. Energy 70, 57-64. https://doi.org/10.1016/S0038-092X(01)00009-3

WeatherSpark, 2025. Climate and Weather Data for Brazil. https://pt.weatherspark.com/countries/BR (accessed 28 March 2025).

Wilcox, S., Gueymard, C., 2010. Spatial and temporal variability of the solar resource in the United States. 39th ASES National Solar Conference 2010 - SOLAR 2010. https://www.researchgate.net/publication/236314614_Spatial_and temporal_variability_of_the_solar_resource_in_the_United States (accessed 31 March 2025).